Current noise spectra of Schottky barrier diodes with electron traps in the active layer

S. Pérez[a] and T. González
Departamento de Física Aplicada, Facultad de Ciencias, Universidad de Salamanca, Plaza de la Merced s/n, 37008 Salamanca, Spain

(Received 22 October 2004; accepted 1 February 2005; published online 23 March 2005)

We present a microscopic analysis of current fluctuations in a GaAs n^+-n-metal Schottky barrier diode containing electron traps in the active layer. An ensemble Monte Carlo simulation is used for the calculations. We analyze the influence of generation-recombination mechanisms of electrons with traps on the current–voltage characteristics and noise spectra of the diode. The presence of traps reduces both the flatband voltage and the current level in the series-resistance regime. With respect to the noise, significant modifications are observed in the current noise spectra. In the barrier-limited regime, while at low-frequency shot noise is not found to change, the returning-carriers peak is strongly modulated by the influence of the traps. Beyond flatband conditions generation-recombination noise becomes evident at low frequency, exhibiting a quadratic dependence on the current. © *2005 American Institute of Physics*. [DOI: 10.1063/1.1879076]

I. INTRODUCTION

The level of low-frequency noise (LFN) is one of the important parameters which determines whether electronic devices are suitable or not for microwave communication systems. It is well known that LFN can translate into unacceptable phase noise at high frequency, which limits the performance of oscillators, mixers, and other electronic systems.[1–3] On the other hand, the analysis of LFN cans be useful not only for improving the device performance but also as a diagnostic tool of device quality and reliability.[4]

The fabrication of high-quality Schottky barrier diodes (SBDs) is necessary to achieve good high-frequency functionality when used as mixers, detectors, or frequency multipliers, and it is also a key aspect for developing various electronic devices such as metal-semiconductor field-effect transistors (MESFETs) and high electron mobility transistors (HEMTs). The analysis of the noise properties of SBDs can provide useful information on the mechanisms controlling transport by means of the knowledge of the nature and location of noise sources.[5–8] In particular, generation-recombination (GR) noise can be used to detect, identify, and locate trap levels at the interface, in the space charge, or in the bulk regions of the diode. This is especially useful for the development of devices based on new materials such as SiC, GaN, etc.[9,10]

SBDs based on typical materials such as Si and GaAs exhibit low levels of LFN when they are used in classical configurations due to its relatively mature technology. But with the development of alternative structures, such as those with quantum dots (QDs) embedded in the active layer, GR mechanisms appear as an important LFN source. QDs are usually fabricated by growing nanometer-sized materials on various substrates. These configurations offer new possibilities of development of transistors, lasers, high efficiency photovoltaic cells, information storage, etc. In particular, the fabrication of InAs QDs grown on GaAs substrates has recently attracted some attention.[5,11,12] GaAs layers are notably modified by the inclusion of QDs, which lead to appearance of a high density of electron traps. The electrical and noise characteristics of QDs embedded in GaAs confining layers are commonly investigated by using SBDs as test devices. The transport and $1/f$ noise properties of these diodes have been experimentally analyzed, finding that the influence of GR mechanisms is extremely important.[5,12] However, a detailed study of the influence of electron traps on the current noise in SBDs at higher frequencies is still not available.

In this paper we analyze the impact of GR processes with electron traps on the static and noise (beyond the $1/f$ range) behavior of the current flowing through a GaAs SBD operating under forward bias in the proximity of flatband conditions. As a first step we consider GR mechanisms only in the volume of the active layer, associated with electron traps characterized by a single energy level. We will focus especially on the dependence of the current noise behavior on the dc bias conditions, trying to identify the signature of the traps in the noise spectra at different frequencies. Different trap densities, locations, and generation and recombination rates will be studied. The Monte Carlo (MC) method is used for the calculations. This technique has been proved to be especially powerful when a microscopic description of the system under investigation is required.[13–21] Hence, we have developed an ensemble MC simulator where GR processes of electrons with traps are implemented coupled with a one-dimensional Poisson solver.

When the diode is biased in the exponential region of the I–V curve we find the outstanding result that even if GR mechanisms do not modify the full shot-noise behavior of the current spectral density at low frequency, they lead to a decrease of the noise at higher frequencies around the returning-carriers peak. Moreover, the voltage at which the transition from the thermionic emission to the series resistance behavior of the diode takes place (this is the applied

[a]Electronic mail: susana@usal.es

voltage needed to reach flatband conditions) changes with the density and characteristics of the traps. Beyond this voltage, GR noise related to the presence of the traps becomes evident also at low frequency. It is precisely around flatband conditions where the SBDs are biased when they operate as mixers and multipliers.[8] Therefore, the previous facts may be considered as an important result to be borne in mind by circuit designers when the optimization of noise properties is one of the keys of the applications.

The paper is organized as follows: In Sec. II the physical system under analysis together with the details of the MC simulation are described. In Sec. III the results obtained for the static characteristics and current noise are reported. Sec. IV summarizes the main conclusions and future trends of our work.

II. PHYSICAL MODEL AND MONTE CARLO SIMULATION

We consider a GaAs n^+-n-metal SBD with dopings $N_D^+ = 10^{17}$ cm^{-3} and $N_D = 10^{16}$ cm^{-3} for the n^+ and n regions, respectively, and the same length for both zones, $l_{n^+} = l_n = 0.35$ μm. The diode is similar to that analyzed in Ref. 19. We consider traps located only in the active n region, because this zone is the major responsible of the diode characteristics, and it is precisely this region that attracted the interest for the fabrication of new structures with embedded QDs.[5–12]

The calculations are performed by using an ensemble MC simulator, one dimensional in real space and three dimensional in momentum space, self-consistently coupled with a one-dimensional Poisson solver. The GaAs microscopic model employed is the same as that used in Ref. 19. The conduction band consists of three nonparabolic spherical valleys (Γ, L, and X). The structure is divided into regular meshes of 100-Å length, with the electric field updated each 2 fs. The cross-sectional area is $A = 4 \times 10^{-13}$ m^2. Simulations are performed at room temperature ($T = 300$ K). The barrier height considered in the simulation is $\Phi_b = 0.737$ V. We assume that Φ_b remains constant with the bias and trap density, since traps are only included in the active n region of the device. The height of the barrier present between the n region and the metal at equilibrium (built-in potential V_{bi}) is equal to 0.639 V in the absence of traps. This barrier is modulated by the instantaneous concentration of trapped carriers. Quantum effects such as tunneling, barrier reflection, and energy lowering of the barrier in the semiconductor-metal contact are not included in the simulation, because our main objective is to provide a detailed analysis of the impact of GR processes in the volume of the active region on the current flowing through the diode.

In our model, free electrons are provided by donor levels close to the bottom of the conduction band, which are completely ionized at the temperature of interest. A single type of electron traps, initially neutral and empty, at a depth E_n below the bottom of conduction band is present in the active n region. It is assumed that the traps interact only with electrons in the conduction band, in such a way that the electrons provided by the donor impurities are distributed over the conduction band and the traps. The electron trapping–detrapping processes are included following the scheme described in Refs. 21 and 22. There are two time constants involved in these processes: the recombination time τ_r (average *free time* of an electron) and the generation time τ_g (average *captured time* of an electron). In the general case of having position-dependent densities of traps $N_t(x)$ and trapped electrons $n_t(x)$, the recombination time depends also on the position, $\tau_r(x)$, and free electrons disappear by trapping at the rate[23]

$$1/\tau_r(x) = N_t(x)\nu_{\mathrm{th}}\sigma\{[N_t(x) - n_t(x)]/N_t(x)\},$$

where $\nu_{\mathrm{th}} = \sqrt{k_B T/m}$ (with k_B the Boltzmann constant and m the electron effective mass) is the thermal velocity of carriers and σ the capture cross section of the traps (as first approximation, assumed to be energy independent in our calculations). In GaAs at 300 K, ν_{th} takes a value of 2.55×10^7 cm/s. In order to implement in the MC simulation this position-dependent recombination probability, we proceed as follows. In those meshes where traps are present, a position-independent probability $1/\tau_r = N_t^{\max}\nu_{\mathrm{th}}\sigma$ is considered to calculate the duration of free flights, $N_t^{\max}$ being the maximum value of $N_t(x)$ along the diode. Once the free flight finishes and the selected mechanism is a trapping process, we determine if it actually takes place by means of the rejection technique according to the probability $[N_t(x) - n_t(x)]/N_t^{\max}$, which accounts for the local density and instantaneous occupancy of traps. To this end, $n_t(x)$ is recalculated every time step. If the carrier is captured, it remains trapped (with null velocity) during a time t_t, which is stochastically selected according to the detrapping probability per unit time $1/\tau_g$. This generation rate is given by $1/\tau_g = \upsilon \exp(-eE_n/k_B T)$, where υ is the attempt-to-escape frequency.[23] When the carrier is released, its velocity components are determined according to a Maxwellian distribution at the lattice temperature.

For the characteristic parameters of traps, initially we have considered a generation time τ_g of 200 ps, a capture cross section σ of 2.61×10^{-13} cm^2, and different trap densities N_t from 5×10^{14} to 10^{16} cm^{-3}, leading to minimum recombination times (when all traps are empty) $\tau_r^{\min} = 1/N_t\nu_{\mathrm{th}}\sigma$ ranging from 0.3 ns to 15 ps. τ_g corresponds to a trap energy $E_n = 0.14$ eV, assuming a typical ν of 10^{12} s^{-1}. The capture cross section considered here is within the highest range measured for deep centers present in GaAs.[24,25] This value of σ, together with the high trap densities, provide lifetimes which are within the lowest ones found in GaAs,[26] thus making computation times affordable.[21]

In a second step we will consider a constant trap density $N_t = 10^{16}$ cm^{-3} and different values of σ and τ_g keeping a constant $\tau_r^{\min}/\tau_g$ ratio of 0.075 (2.61×10^{-13} cm^2, 200 ps; 5.22×10^{-13} cm^2, 100 ps; and 2.61×10^{-12} cm^2, 20 ps).

The high values of electron traps considered in this work allow identifying clearly the associated effects both in the $I-V$ curve and in the current noise. Note that the highest value considered for N_t is the same as the doping of the n region. This extreme is not typically reached in standard SBDs, where the effects described in this work should not be expected. However, in SBDs embedding new layers to fab-

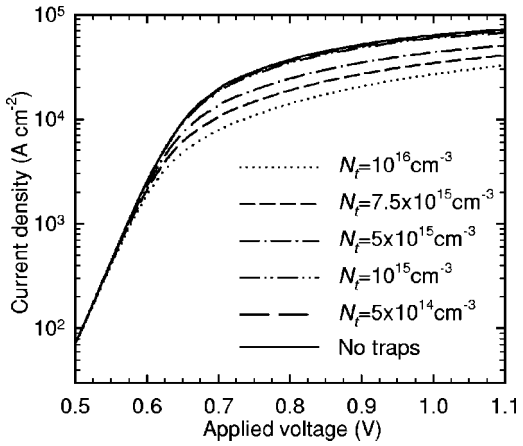

FIG. 1. Current–voltage characteristics of the SBD under forward-bias conditions obtained with trap densities varying from 5×10^{14} to 10^{16} cm^{-3}. $\sigma=2.61\times10^{-13}$ cm^2 and $\tau_g=200$ ps. The solid line corresponds to the absence of traps.

ricate QDs, very high densities of traps and defects can be present (due to the distortion of the bonds in the capping GaAs layer).[5,11,12]

The device is biased by a constant voltage V and we calculate the instantaneous current $I(t)$ that passes through the diode. We quantify the average value of this current (static $I-V$ characteristic) and its fluctuations (noise analysis). The noise analysis is performed by means of the calculation of $S_I(f)$, the spectral density of current fluctuations, obtained by Fourier transform of the corresponding autocorrelation function $C_I(t)$, directly evaluated from the instantaneous current values provided by the simulations.[13]

III. RESULTS

In this section we analyze the influence of trapping–detrapping processes, first on the static $I-V$ characteristics and then on the noise behavior of the diode, as a function of the density, occupancy, location, and characteristic parameters of traps.

A. Static characteristics

The current–voltage semilog characteristics under forward-bias conditions are shown in Fig. 1 for $\tau_g=200$ ps, $\sigma=2.61\times10^{-13}$ cm^2, and several values of trap density N_t in the active region. The solid line represents the $I-V$ characteristic when no traps are considered. Due to the presence of the barrier, only voltages higher than 0.5 V can be reliably simulated.[19] In each curve, two main transport regimes that characterize the SBD behavior can be distinguished. The first one, for low voltages, is the barrier-limited regime, where thermionic emission over the barrier is responsible for the current, which exhibits an exponential dependence on the applied voltage V. The second one is the series resistance regime, which occurs for higher voltages when there is no longer a barrier, and a linear $I-V$ dependence is observed. The value of the applied voltage at which the transition between both regimes takes place (flatband voltage V_{FB}) changes with the trap density, decreasing as N_t increases. As follows from Fig. 1, under barrier-limited regime the current

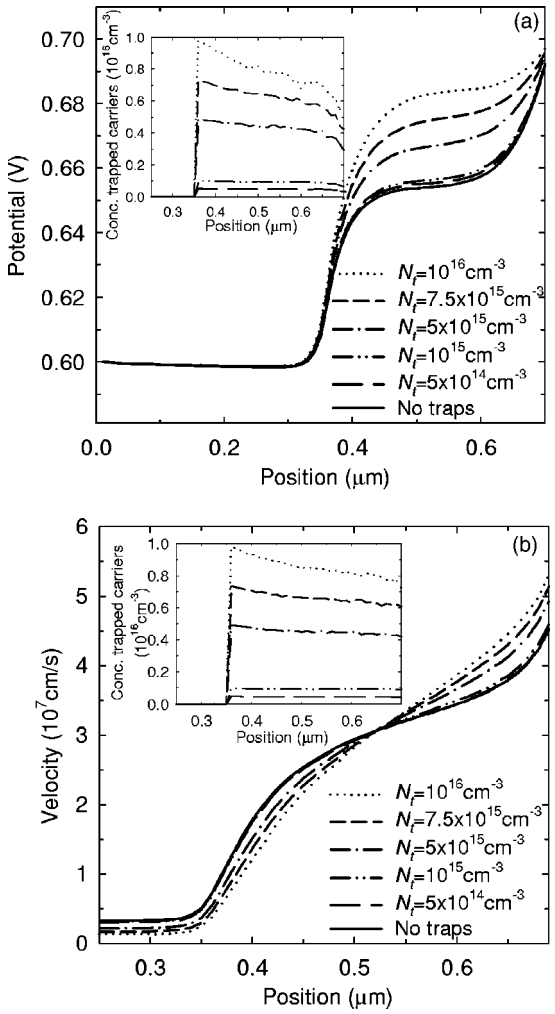

FIG. 2. Stationary profiles of (a) potential at $V=0.6$ V and (b) velocity at $V=0.9$ V obtained with trap densities varying from 5×10^{14} to 10^{16} cm^{-3}. $\sigma=2.61\times10^{-13}$ cm^2 and $\tau_g=200$ ps. The solid line corresponds to the absence of traps. The insets show the corresponding concentration of trapped carriers.

is independent of N_t in spite of the modulation that the trapped charge induces on the barrier height present between the n region and the metal [see Fig. 2(a)]. Since traps are only present in the active n region (interface traps are not included in the model), the total barrier that electrons injected at the ohmic contact in the n^+ region must overcome to reach the metal at the Schottky contact is not affected by trapped electrons, and therefore the total overage current found in this regime is independent of N_t. In contrast, trapped charge has a severe effect on the electrical behavior at high voltages beyond flatband. Due to the lower free-electron concentration present in the n region as N_t increases, SBDs exhibit a larger series resistance R_S that leads to lower values of the current and, as it will be shown later, changes the noise level of the device. It is interesting to note that in applications such as mixers and multipliers, SBDs are usually biased around flatband conditions; therefore, the changes in the flatband voltage (and in the electrical behavior above it) associated to the presence of traps must be taken in mind by circuit designers. Similar differences in the $I-V$ characteristics are obtained when the trap density is kept constant and the ratio between τ_r and τ_g is modified.

Figure 2 shows the stationary profiles along the structure of (a) electric potential for a voltage bias when the semiconductor-metal barrier persists ($V=0.6$ V) and (b) average electron velocity beyond flatband conditions ($V=0.9$ V), for the same parameters as those used in the previous figure. The insets of Fig. 2 show the density of trapped carriers inside the n region of the device for each bias. For the lowest values of N_t, near all the traps are occupied, thus compensating a fraction of the positive charge associated to the ionized donors. However, due to the small value of N_t, as compared to the doping of the n region N_D, the trapped charge has a very small influence on the profiles of potential and velocity. When the density of traps increases not all the traps are occupied. The fraction of free traps is higher near the metal contact, especially for $V=0.6$ V due to the presence of the depletion region. In this case, due to the significant density of negative trapped charge as compared to N_D, the potential and velocity profiles are noticeably affected.

For applied voltages lower than V_{FB}, the barrier between the n region and the metal persists, as observed in Fig. 2(a); its value depending on the trap density. Due to the significant compensation of positive fixed charge originated by the trapped electrons, the built-in potential between the n^+ and n regions increases with N_t. Since the potential difference between both metal contacts is the same in all cases (no interface traps are considered), the barrier between the n region and the metal decreases for increasing N_t. This is also the reason for the decrease of V_{FB} observed in Fig. 1. For applied voltages below V_{FB} the current is the same for the different values of N_t since, as long as the barrier is present and the free carrier concentration in the n^+ region is the same, the current depends only on the potential difference between the terminals (and not on how it is spatially distributed). In the case of $V>V_{FB}$ it is interesting to analyze the stationary profiles of velocity. For low N_t, they are similar to that found in the absence of traps. However, for higher values of N_t, the redistribution of the electric-field profile originated by the trapped negative charge leads to an increase of the peak velocity near the metal contact, while reducing its value near the n^+-n junction. As N_t increases, higher velocity carriers reach the metal contact. This fact will have a strong influence on the noise characteristics of the device that will be described later.

The distortion of the electric-field profile originated by the presence of the trapped negative charge is better observed in Fig. 3, where the influence of the trap location on the electric-field and velocity profiles is illustrated for $V>V_{FB}$. To this end, we consider the presence of a trap density $N_t=10^{16}$ cm^{-3} only in some specific zones of the active n region. For the simulation, the device is divided into meshes of 100 Å each, 35 of them corresponding to the n region. We consider the presence of traps in seven zones formed of five consecutive meshes, going from the boundary with the n^+ region (zone 1) to the vicinity of the metal contact (zone 7). In Fig. 3(a) it is observed that the distortion of the electric field originated by the trapped negative charge, though more pronounced around the location of the traps, extends to practically all the active region due to the short length of the diode. When traps are located in the middle of the n region

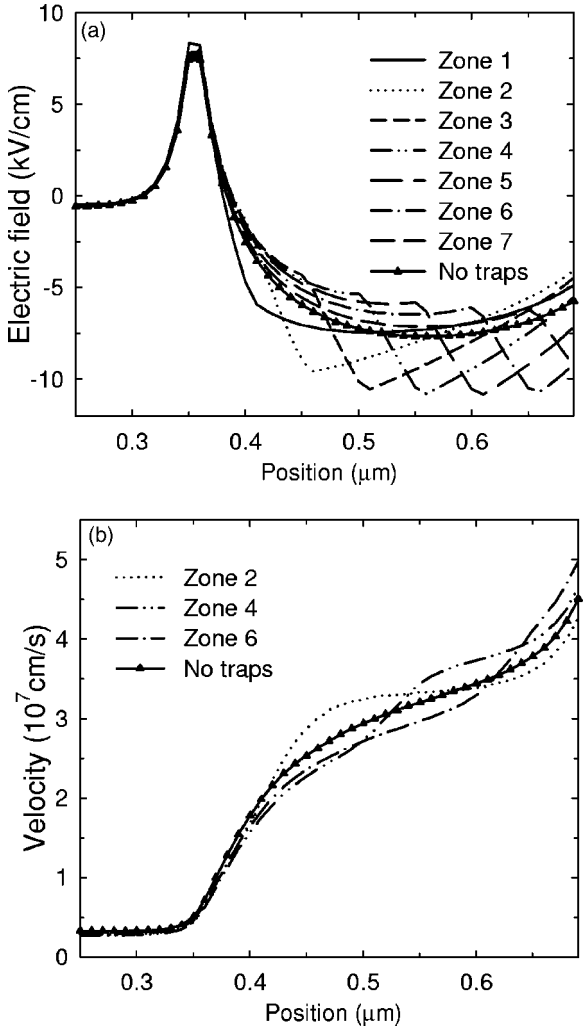

FIG. 3. Stationary profiles of (a) electric field and (b) velocity for several trap locations of equal size in the n region going from zone 1 in the proximity of the n^+ region to zone 7 by the metal. $N_t=10^{16}$ cm^{-3}, $\sigma=2.61\times10^{-13}$ cm^2, $\tau_g=200$ ps, and $V=0.9$ V. The solid line with triangles corresponds to the absence of traps.

(zone 4, around 0.525 μm) the electric-field distortion is more important and extends over a wider length. Indeed, for traps in zones 4, 5, and 6 it is when the average current beyond flatband conditions is more affected by the presence of the traps, decreasing in value with respect to the case when traps are absent. As observed in Fig. 3(b), the profile of average carrier velocity is substantially modified by the location of traps, fact which has important influence on the noise behavior.

B. Current noise

Figure 4 shows the low-frequency (beyond the $1/f$ range) current noise spectral density $S_I(0)$ as a function of the forward current I for the same trap densities and associated parameters as those considered in the static study. The solid lines correspond to $2qI$ and $\propto I^2$ dependences, plotted for comparison. As follows from the figure, in the low current region (corresponding to $V<V_{FB}$) the value of $S_I(0)$ corresponds to the typical full shot-noise behavior $[S_I(0)=2qI]$ caused by carriers crossing the barrier individually

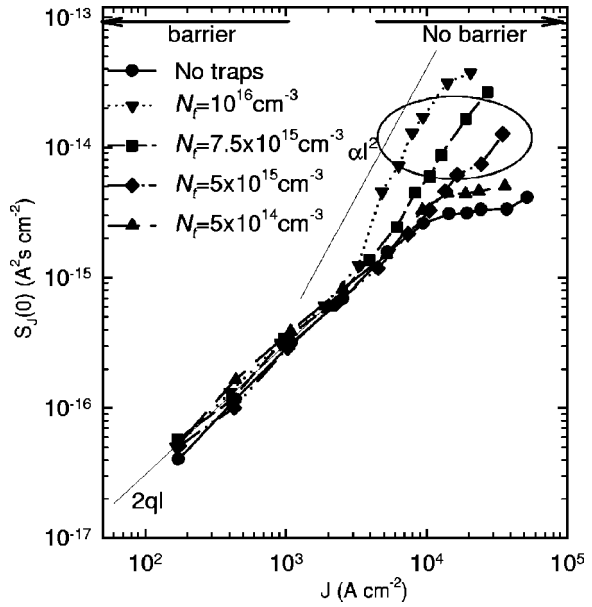

FIG. 4. Low-frequency value of the current spectral density as a function of the forward current for several values of trap concentration. $\sigma=2.61\times10^{-13}$ cm^2 and $\tau_g=200$ ps. The solid line with circles corresponds to the absence of traps. $2qI$ and $\propto I^2$ behaviors are plotted for comparison.

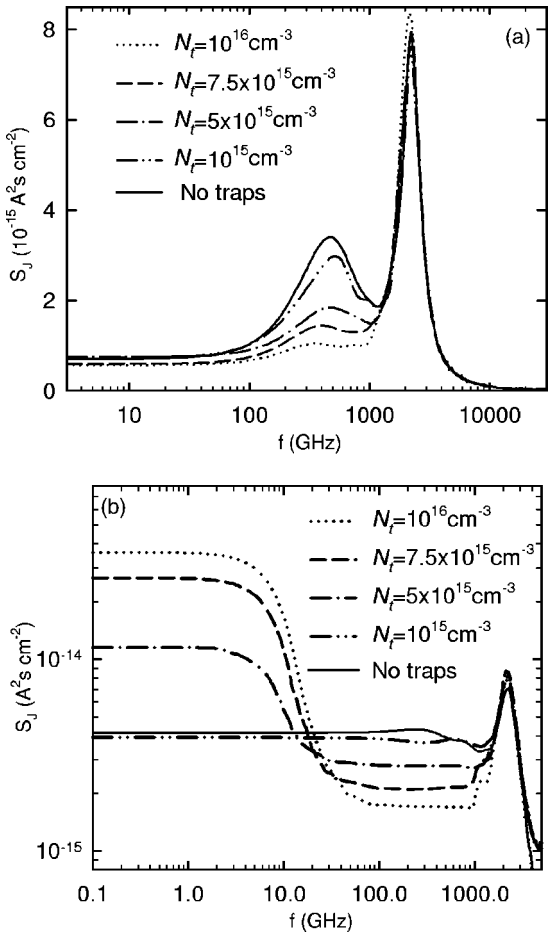

FIG. 5. Spectral density of current fluctuations as a function of frequency for (a) $V=0.6$ V and (b) $V=0.9$ V, and several values of trap concentration. $\sigma=2.61\times10^{-13}$ cm^2 and $\tau_g=200$ ps. The solid line corresponds to the absence of traps.

and at random. This noise level is the same as that obtained in the absence of the traps. This result indicates that as long as the barrier persists and determines the current flowing though the diode, the low-frequency value of the spectral density does not show any influence of the GR mechanisms, shot noise being dominant.

In contrast, for high forward currents (corresponding to $V>V_{FB}$) $S_I(0)$ exhibits the clear signature of GR noise. In the absence of traps (and for low trap densities) $S_I(0)$ approaches a value close to $4k_BT/R_S$, corresponding to the thermal noise associated with the series resistance R_S, which limits the current in this range.[19] When traps are present, a significant increase of $S_I(0)$ proportional to I^2 (typical of GR noise) is observed in the diodes that contain the highest trap densities, more pronounced the higher the value of N_t. This fact indicates that the main contribution to the total noise in this range originates from fluctuations in the carrier number due to the trapping–detrapping processes, which prevail over the noise associated with the series resistance. As expected from the decrease of V_{FB} observed for increasing N_t, the transition from shot noise to excess GR noise behaviors in $S_I(0)$ takes place for lower current values the higher is N_t. It must be pointed out that both the $I-V$ and the $S_I(0)$-V curves show substantial deviations from the case in which traps are absent when the distortion of the electric field in the active n region originated by the presence of trapped electrons is strong enough to appreciably modify the velocity of electrons when reaching the metal contact. In our calculations this happens for $N_t\geqslant5\times10^{15}$ cm^{-3} [see Fig. 2(b)].

Once the low-frequency behavior of current noise has been explained, in Fig. 5, we show the dependence of the spectral density on frequency $S_I(f)$ in the two regimes of operation of the SBD for the different values of trap density. Figure 5(a) corresponds to $V=0.6$ V and Fig. 5(b) to $V=0.9$ V. In both regimes a peak at high frequency around 2 THz appears. This peak is related to the plasma oscillation frequencies of the n^+ and n regions.[19] Its magnitude and frequency depend essentially on the doping and length of these regions.[27] Thus, the peak is practically independent of the bias conditions and trap density.

For $V<V_{FB}$, in the presence of the barrier, a second peak placed about 600 GHz is present. This peak is attributed to the so-called *returning carriers*, carriers that do not have enough energy to surmount the barrier with the metal and thus come back to the neutral semiconductor. As explained in the discussion of Fig. 2(a), the barrier present between the n region and the metal decreases when the trap density increases. The amplitude and frequency of the returning-carriers peak tend to decrease when such a barrier is lower,[28] which is just the behavior observed in Fig. 5(a) for increasing N_t. This is an outstanding result; even if in the barrier-limited regime neither the dc behavior nor the LFN reflect the influence of the presence of traps [for a given applied voltage both I and $S_I(0)$ do not depend on N_t], at intermediate frequencies the level of noise becomes reduced. We remark that this happens as result of the modification of the electrical characteristics of the diode (lowering of the n region-metal barrier height) due to the trapped negative charge and not because of the introduction of an additional source of noise, such as GR processes.

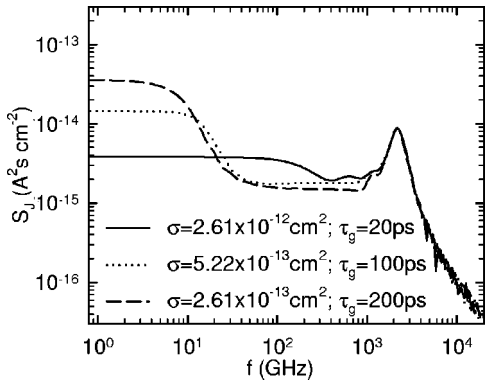

FIG. 6. Spectral density of current fluctuations as a function of frequency for a constant trap density $N_t=10^{16}$ cm^{-3} and different sets of values of σ and τ_g (2.61×10^{-13} cm^2, 200 ps; 5.22×10^{-13} cm^2, 100 ps; and 2.61×10^{-12} cm^2, 20 ps) that provide the same $\tau_r^{\min}/\tau_g$ ratio of 0.075, thus leading to a similar density of trapped carriers. $V=0.9$ V.

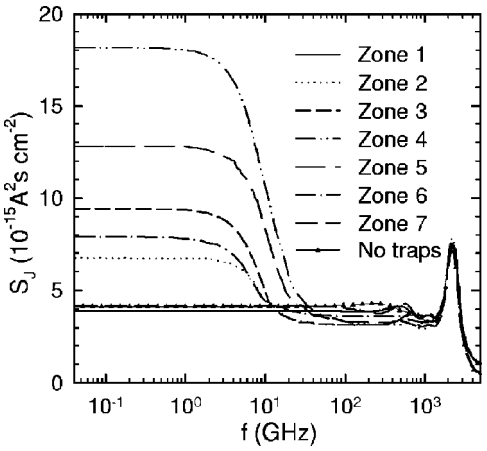

FIG. 7. Current spectral density for several trap locations of equal size in the n region going from zone 1 in the proximity of the n^+ region to zone 7 by the metal. $N_t=10^{16}$ cm^{-3}, $\sigma=2.61\times10^{-13}$ cm^2, $\tau_g=200$ ps, and $V=0.9$ V. The solid line with triangles corresponds to the absence of GR processes.

The spectra change significantly if the diode is biased in the series resistance regime, as observed in Fig. 5(b) for $V=0.9$ V. Here, as expected, the peak at intermediate frequencies related to the returning carriers disappears. In the absence of traps (and for low trap densities), the main contribution to $S_I(f)$ in this regime at low and intermediate frequencies (before plasma effects) is associated to the series resistance: $S_I(f)$ in this region is essentially given by $4k_BT/R_s$. When high trap densities are present, a low-frequency GR contribution to the noise is expected. Such a contribution, clearly evidenced in Fig. 5(b), exhibits a Lorentzian dependence on frequency and is more pronounced the higher is N_t, as already observed in Fig. 4. The corresponding corner frequency is related to the characteristic parameters of the trapping-detrapping processes and to the density and occupancy of the traps, being of the order of $f_t=1/2\pi\tau_\ell$, with $\tau_\ell=\tau_r\tau_g/(\tau_r+\tau_g)$,[21,23] which, for the case of $N_t=10^{16}$ cm^{-3} (and taking $\tau_r=\tau_r^{\min}=1/N_t\nu_{\text{th}}\sigma$, i.e., neglecting the influence of trap occupancy), provides $f_t=11.4$ GHz, close to the MC value. As N_t decreases, the cutoff of the GR contribution takes place at lower frequencies, as observed in Fig. 5(b). Beyond the GR contribution and before the plasma peak there is a range of intermediate frequencies where, in the absence of returning carriers, thermal noise related to the series resistance becomes dominant. Here, lower noise levels are observed as N_t becomes higher, consistently with the increase of R_s with N_t already explained and detected in the static $I-V$ curves of Fig. 1.

To better illustrate the dependence of the GR noise contribution on the characteristic parameters of the trapping–detrapping processes, Figure 6 shows the current noise spectra calculated for a constant trap density $N_t=10^{16}$ cm^{-3} and three sets of values of σ and τ_g (2.61×10^{-13} cm^2, 200 ps; 5.22×10^{-13} cm^2, 100 ps; and 2.61×10^{-12} cm^2, 20 ps) that lead to the same $\tau_r^{\min}/\tau_g$ ratio of 0.075, so that a very similar trap occupancy is present in the three cases. This means that the density of trapped carriers, the value of the series resistance R_s and the current flowing through the diode are practically the same for the three sets of parameters, and the differences appearing in the noise spectra are only related to the GR kinetics. Assuming a standard GR noise spectra, one would expect to find $S_I(f)\propto\tau_\ell I^2/(1+2\pi f^2\tau_\ell^2)$. This is confirmed by the results shown in Fig. 6, where the low-frequency value of the GR contribution and the cutoff frequency are observed to be proportional and inversely proportional to τ_ℓ; respectively. Since R_s is similar in the three cases, the level of thermal noise obtained at intermediate frequencies is also very similar.

In order to optimize the technological processes of fabrication of SBDs it is interesting to analyze the influence of trap location on the current noise. To this end, we will consider traps present only in some specific zones of the active region, as described in the discussion of Fig. 3 in the previous section. Results are depicted in Fig. 7. In the case of traps placed close to the n^+ region (zone 1) or by the metal (zone 7), the electric-field profile is not strongly affected by the presence of trapped electrons [Fig. 3(a)], and the spectrum is not substantially modified with respect to the absence of traps. The low-frequency plateau of GR noise becomes evident in the diodes in which traps are located in intermediate zones of the active region, being more pronounced the closer are the traps to the middle of the n region (zone 4). As observed in Fig. 3(a), in these cases the distortion of the electric field extends over a wide part of the active region, leading to an increase of carrier velocity that reaches the metal contact [Fig. 3(b)] and couples number fluctuations in the active region with current fluctuations at the contacts.

IV. CONCLUSIONS

An ensemble MC simulation has been used to investigate the static characteristics and noise spectra of a GaAs SBD where GR processes of electron with traps are included in the active n region of the diode. Two main behaviors are distinguished depending on the operating point. In the exponential region of the $I-V$ characteristics, no influence of GR processes on the noise are observed at low frequency, but an important noise reduction at higher frequencies around the returning-carriers peak takes place. In the series resistance regime, a Lorentzian GR contribution increases the level of noise at low frequency, whose amplitude and corner fre-

quency depend on the characteristic parameters of the traps and their density. We have shown that the major contribution to the current noise at the terminals is originated by the traps placed in the middle of the active region. The level of thermal noise at intermediate frequencies is reduced when the density of traps increases due to the associated reduction of the series resistance. The flatband voltage also changes with the trap density. These results are relevant for modern SBD structures embedding QDs in the active region, which lead to high densities of electron traps.

Finally, we remark that in this work we have not included the influence of interface traps that could change the value of the barrier height (kept constant in our calculations). The study of the influence of surface traps and associated GR processes will be the objective of forthcoming works.

ACKNOWLEDGMENTS

The authors gratefully acknowledge helpful discussions with Professor D. Pardo and Dr. J. Mateos. This work has been partially supported by Project No. TIC2001-1754 from the Dirección General de Investigación (and FEDER) and Project No. SA57/02 from the Consejería de Educación y Cultura de la Junta de Castilla y León.

[1]H. Siweris and B. Schieck, IEEE Trans. Microwave Theory Tech. **33**, 233 (1985).
[2]M. N. Tutt, D. Pavlidis, A. Khatizadeh, and B. Bayraktaroglu, IEEE Trans. Microwave Theory Tech. **43**, 1461 (1995).
[3]H. Darabi and A. A. Abidi, IEEE J. Solid-State Circuits **33**, 15 (2000).
[4]L. K. J. Vandamme, IEEE Trans. Electron Devices **41**, 2176 (1994).
[5]N. A. Hastas, C. A. Dimitriadis, L. Dozsa, E. Gombia, S. Amighetti, and P. Frigeri, J. Appl. Phys. **93**, 3990 (2003).
[6]S. Palczewski, A. Jelenski, A. Grub, and H. L. Hartnagel, IEEE Microw. Guid. Wave Lett. **2**, 442 (1992).
[7]H. Arakaki, K. Ohashi, and T. Sudou, Semicond. Sci. Technol. **19**, 127 (2004).
[8]A. Jelenski, A. Grub, V. Krozer, and H. L. Hartnagel, IEEE Trans. Microwave Theory Tech. **41**, 549 (1993).
[9]L. Anghel, T. Ouisse, T. Billon, P. Lassagne, and C. Jaussaud, Diamond Relat. Mater. **6**, 1494 (1997).
[10]S. L. Rumyantsev *et al.*, IEEE Trans. Electron Devices **48**, 530 (2001).
[11]I. Tanaka, I. Kamiya, H. Sakaki, N. Qureshi, S. J. Allen, and P. M. Petroff, Appl. Phys. Lett. **74**, 844 (1999).
[12]N. A. Hastas, D. H. Tassis, C. A. Dimitriadis, L. Dozsa, S. Franchi, and P. Frigeri, Semicond. Sci. Technol. **19**, 461 (2004).
[13]L. Varani, L. Reggiani, T. Kuhn. T. González, and D. Pardo, IEEE Trans. Electron Devices **41**, 1916 (1994).
[14]G. Hill, P. N. Robson, and W. Fawcett, J. Appl. Phys. **50**, 356 (1979).
[15]R. Fauquembergue, J. Zimmermann, A. Kaszynski, E. Constant, and J. P. Nougier, J. Appl. Phys. **51**, 1065 (1980).
[16]J. G. Adams, T.-W. Tang, and L. E. Kay, IEEE Trans. Electron Devices **41**, 575 (1994).
[17]T. González, D. Pardo, L. Varani, and L. Reggiani, IEEE Trans. Electron Devices **42**, 991 (1995).
[18]M. J. Martín, D. Pardo, and J. E. Velázquez, J. Appl. Phys. **84**, 5012 (1998).
[19]T. González, D. Pardo, L. Reggiani, and L. Varani, J. Appl. Phys. **82**, 2349 (1997).
[20]J. Mateos, T. González, D. Pardo, V. Hoel, and A. Cappy, Semicond. Sci. Technol. **14**, 864 (1999).
[21]S. Pérez, T. González, S. L. Delage, and J. Obregon, J. Appl. Phys. **88**, 800 (2000).
[22]B. G. Vasallo, J. Mateos, D. Pardo, and T. González, Fluct. Noise Lett. **2**, L243 (2002).
[23]A. van der Ziel, *Solid State Physical Electronics* (Prentice Hall, New Jersey, 1976).
[24]K. Shenai and R. W. Dutton, IEEE Trans. Electron Devices **35**, 590 (1988).
[25]D. Bimberg, H. Münzel, A. Steckenborn, and J. Christen, Phys. Rev. B **31**, 7788 (1985).
[26]S. Dannefaer, P. Mascher, and D. Kerr, J. Phys.: Condens. Matter **1**, 3213 (1989).
[27]L. Reggiani, P. Golinelli, E. Faucher, L. Varani, T. González, and D. Pardo, *Proceedings of the 13th International Conference on Noise in Physical Systems and* $1/f$ *Fluctuations*, edited by V. Bareikis and R. Katilius (World Scientific, Singapore, 1995), pp. 163–168.
[28]M. Trippe, G. Bosman, and A. van der Ziel, IEEE Trans. Microwave Theory Tech. **MTT-34**, 1183 (1986).